On the Possibility of a Pseudo Atomic Ground State for CrF_2: Ab-Initio and Crystal Field Calculations Including Spin−Orbit Coupling

Carl Ribbing,* Birgit Dumez, Arnout Ceulemans, and Kristine Pierloot

Division of Quantum Chemistry, University of Leuven, B-3001 Leuven, Belgium

Received: March 5, 1997; In Final Form: May 28, 1997[⊗]

Ab-initio and crystal field calculations including spin−orbit coupling suggest that the ground state of the CrF_2 complex might have characteristics of an atomic type ground state. It is shown that the crossing of the $^5\Sigma^+$ and $^5\Pi$ can be compared to a ^{5}P spin−orbit split atomic state.

1. Introduction

In a recent review paper of nonadiabatic effects in spectroscopy and chemical reactions, it has been shown that conical intersections probably are far more common in molecular systems than was expected a couple of years ago.[1]

In the course of systematic ab-initio investigations of the transition metal difluorides from ScF_2 to CuF_2,[2] two cases were found where spin−orbit coupling effects seemed to be of importance for the ground state: CrF_2 and CoF_2. The investigations showed that CrF_2 might have a triple conical intersection connected to its ground state, as a result of a level crossing of a $^5\Pi$ and a $^5\Sigma^+$ state.

In the present paper we discuss the CrF_2 results, which show that this peculiar level crossing may give rise to a pseudo atomic ground state. Experimentally it has not been possible to determine if the molecule in gas phase is linear or bent.[3] The ab-initio results we present in this paper could be helpful for further experimental studies.

We use extensive correlation treatment together with an effective spin−orbit coupling operator to calculate the $^5\Sigma^+$, $^5\Pi$, and $^5\Delta$ states and the spin−orbit interactions between them. The one-dimensional potential curve along the symmetric stretch with and without spin−orbit coupling is presented, and the implications for the ground state are discussed.

A crystal field type calculation of the spin−orbit couplings is also presented. The spin−orbit splitting pattern can be explained in terms of pseudo angular momenta of the d-orbitals.

2. Computational Details

a. Ab-Initio Calculations. CASSCF and CASPT2 calculations were performed with the MOLCAS program package.[4] We employed ANO type basis sets of the following sizes, Cr: (17s12p9d4f/7s6p4d2f)[5] and F:(14s9p4d3f/5s4p2d1f).[6] For details on the optimization of the basis sets, see refs 5 and 6.

We tried four different levels of computation. The same CASSCF active space was used in all calculations, four electrons in five orbitals: (I) CASPT2 correlating the 3d electrons on Cr and the 2s and 2p electrons on F; (II) CASPT2 correlating 3s, 3p, and 3d on Cr and 2s and 2p on F (III) and (IV) same as in methods I and II but adding relativistic mass-velocity and Darwin corrections obtained at the CASSCF level. From these four different types, method IV was chosen for reasons discussed in the following section.

For a selected set of symmetric Cr−F distances we calculated the CASSCF, CASPT2 energies with method IV, for three components in D_{2h} symmetry $^5\Sigma^+ = {}^5A_g$, $^5\Pi_a = {}^5B_{2g}$, and $^5\Delta_a = {}^5B_{1g}$. This gives the excitation energies before spin−orbit coupling.

The CASSCF wave function optimized for one component of degenerate states does not necessarily transform according to the irreducible representation of $D_{\infty h}$. This symmetry breaking can be partly avoided by the supersymmetry option in the CASSCF program. The orbitals then form reducible representations in $D_{\infty h}$ of the same dimension as the number of orbitals in each representation. Under the $D_{\infty h}$ symmetry operations, orbitals within the same representation mix but orbitals of different representations do not.

For the spin−orbit coupling calculations one unique set of orbitals for each distance was needed. Separate CASSCF calculations for each component of all states were performed. The $^5\Pi$ and the $^5\Delta$ states have two components and the $^5\Sigma^+$ state has one, which results in five CASSCF wave functions. Since these orbitals do not differ very much we could average the five sets to one, by averaging the respective density matrices. In this way all the correct degeneracies of $D_{\infty h}$ were obtained.

The spin−orbit operator can be introduced at various levels of approximation; see refs 7 and 8 and references therein. Here, we have chosen a simple one-center one-electron operator with an effective charge scaled to reproduce experimental ionic splittings of the heavy center. The one-center character of the spin−orbit coupling is due to the closed shell structure of the fluorine ligands and the ionic structure of the CrF_2. The ionic structure is evident from the Mulliken composition analysis of the 3d-type orbitals; here the percentage is at most 2% F mixing into the Cr 3d-orbitals. Therefore spin−orbit coupling through F^- must include either exciting F^- or charge transfer from F^- to Cr^{2+}. Both of these processes are high in energy and thus do not contribute to the lower states. The spin−orbit operator is

$$\hat{H}_{so} = Z_{eff}\frac{\alpha^2}{2}\sum_i\left[\frac{1}{r^3}\hat{l}_i\cdot\hat{s}_i\right] \qquad (2.1)$$

Z_{eff} is the effective charge of the heavy center and is determined by comparing experimental and calculated atomic splittings. In our case the first order spin−orbit splitting of the $^5D(d^4)$ ground state of Cr^{2+} was chosen. With the same basis set as for the CrF_2 calculations, we calculated the spin−orbit coupling matrix elements inside the $^5D(d^4)$ multiplet. The best matching splitting was obtained with an effective charge of 14.0.

The value of the effective charge may seem large. The reason is that the largest contribution to the spin−orbit integrals comes from the region close to the nucleus because of the $1/r^3$ dependence. Our spin−orbit operator partly lacks the two-

[⊗] Abstract published in *Advance ACS Abstracts,* July 1, 1997.

S1089-5639(97)00840-2 CCC: $14.00

TABLE 1: Symmetries of the Spin−Orbit Components under the D_∞ Double Group

state	orbital	⊗	spin			=	spin−orbit					
$^5\Sigma^+$	Σ^+		Σ^+	Π	Δ		Σ^+	Π	Δ			
$^5\Pi$	Π		Σ^+	Π	Δ		Σ^+	2Π	Δ	Σ^-	Φ	
$^5\Delta$	Δ		Σ^+	Π	Δ		Σ^+	Π	Δ	Σ^-	Φ	Γ

electron part from the Breit−Pauli operator. The difference between the real charge 24 and the effective 14 can be explained as the screening of the nucleus by core electrons. The number of core electrons is $1s^22s^22p^63s^23p^6 = 18$, so it might be expected that the effective charge would be about 6. However due to the fact that the d-orbitals penetrate the charge cloud all the way to the nucleus and the $1/r^3$ factor in the spin−orbit operator, the resulting screening is smaller and the effective charge is larger.

In the correlated calculations it is possible to introduce spin−orbit coupling in various ways (see ref 8 and references therein). Most experience points to the fact that the correlation energy is usually more difficult to calculate than the spin−orbit coupling. In CrF_2 we assume that the spin−orbit coupling is small enough to exclude interactions with higher excited states other than the $^5\Sigma^+$, $^5\Pi$, and $^5\Delta$.

The spin−orbit coupling matrix elements were calculated from a CAS type CI expansion of Slater determinants in the d-orbital space. The eigenvectors from this small CI expansion form the basis of the spin−orbit coupling matrix ($^5\Sigma^+$, $^5\Pi$, and $^5\Delta = 25$ states). In this matrix the diagonal elements give the vertical excitation energy without spin−orbit coupling. These energies are not very accurate. Therefore these were substituted with the more accurate CASPT2 results. Diagonalizing the resulting 25×25 matrix gave us the eigenvectors and eigenvalues corresponding to the double-group spin−orbit states of $D_{\infty h}$ expressed in the basis of the $^5\Sigma^+$, $^5\Pi$, and $^5\Delta$ states.

To assign the eigenvectors to the different double-group representations, we used the fact that different irreducible double-group representations mix only certain spin states. This can clearly be seen in Table 1. For example the spin−orbit state Δ consists of components from each of $^5\Sigma^+$, $^5\Pi$, and $^5\Delta$, while Σ^- is a mixture of only $^5\Pi$ and $^5\Delta$ components. Sometimes, however, it was necessary to look into the coefficients of the wave function to distinguish, for example, Σ^+ and Π.

b. Crystal Field Calculations. For a better understanding of the spin−orbit results, additional crystal field calculations were performed on the manifold formed by the $^5\Pi$ and $^5\Sigma^+$ states. These states were constructed from Slater determinants including the four valence electrons. The $^5\Delta$ state was excluded as compared to the above ab-initio calculations.

The valence orbitals were defined as $(2z^2 - x^2 - y^2)$, (yz), (xz), (xy), and $(x^2 - y^2)$. The d^4-configuration gives rise to an atomic ^5D term that resolves into $^5\Sigma^+ + {}^5\Pi + {}^5\Delta$ cylindrical terms. To calculate the spin−orbit interactions, let us define the following Slater determinants of d-orbitals all with spin projection $M_s = 2$.

$$|\Pi_a\rangle = |(xy)\,(x^2 - y^2)\,(xz)\,(2z^2 - x^2 - y^2)\rangle$$

$$|\Pi_b\rangle = |(xy)\,(x^2 - y^2)\,(yz)\,(2z^2 - x^2 - y^2)\rangle \qquad (2.2)$$

$$|\Sigma\rangle = |(xy)\,(x^2 - y^2)\,(xz)\,(yz)\rangle$$

It is not necessary to calculate all the spin projections $M_s = 2$, 1, 0, −1, −2. Instead we can use the Wigner−Eckart theorem[7,9] and write the spin−orbit operator in a form with suitable transformation properties. Thus we make a decomposition of the spin−orbit operator into components with symmetry adaption to the rotational group.[9]

$$\hat{H}_{so} = \lambda\left(\frac{1}{\sqrt{2}}[i\hat{T}^1_y - \hat{T}^1_x + i\hat{T}^{-1}_y + \hat{T}^{-1}_x] + \hat{T}^0_z\right) \qquad (2.3)$$

with

$$\hat{T}^1_a = -\frac{1}{\sqrt{2}}\hat{L}_a(\hat{S}_x + i\hat{S}_y)$$

$$\hat{T}^0_a = \hat{L}_a\hat{S}_0 \qquad (2.4)$$

$$\hat{T}^{-1}_a = \frac{1}{\sqrt{2}}\hat{L}_a(\hat{S}_x - i\hat{S}_y)$$

$\hat{L}_a$ is the Cartesian orbital angular momentum operator and $\hat{S}_m$ is the spin operator in spherical basis. The Wigner−Eckart theorem is now used to achieve a relation between the matrix elements and a quantity known as the reduced matrix element. The general expression for matrix elements in a basis of eigenfunctions of $\hat{S}^2$ and $\hat{S}_z$ is

$$\langle S,M_s,E|\hat{T}^m_a|S',M'_s,E'\rangle = (-1)^{(S-M_s)}\begin{pmatrix} S & 1 & S' \\ -M_s & m & M'_s \end{pmatrix}\langle S,E||\hat{T}_a||S',E'\rangle \qquad (2.5)$$

where $\langle S,E||\hat{T}_a||S',E'\rangle$ is the reduced matrix element without any dependence of the M_s. The matrix elements expressed in this form greatly simplify the calculations since the spin symmetry can be separated out from the problem and is contained in the 3-J symbol. In total there are only three reduced matrix elements that need to be evaluated.

$$\langle 2,\Pi_a||T_z||2,\Pi_b\rangle\, w = \langle 2,2,\Pi_a|T^0_z|2,2,\Pi_b\rangle = -2\lambda i$$

$$\langle 2,\Pi_a||T_x||2,\Sigma^+\rangle\, w = \langle 2,2,\Pi_a|T^0_x|2,2,\Sigma^+\rangle = 2\lambda i\sqrt{3} \qquad (2.6)$$

$$\langle 2,\Pi_b||T_y||2,\Sigma^+\rangle\, w = \langle 2,2,\Pi_b|T^0_y|2,2,\Sigma^+\rangle = 2\lambda i\sqrt{3}$$

$$w = \begin{pmatrix} 2 & 1 & 2 \\ -2 & 0 & 2 \end{pmatrix} = \sqrt{\frac{2}{15}} \qquad (2.7)$$

Here we note the interesting fact that there is a geometrical factor differing in the matrix elements. The factor of $\sqrt{3}$ is a consequence of the spherical harmonic d-functions. The π and the σ^+ orbitals can be represented either as Y^2_1, Y^2_{-1}, and Y^2_0 or xz, yz, and $2z^2 - x^2 - y^2$. See refs 10−12 for discussions of the properties of the real solid and spherical harmonics.

Since we are interested in an explanation of the spin−orbit effects all the Coulomb interactions were included as diagonal elements in the Hamiltonian, the same way as above. In total we have three parameters: the energies of the $^5\Sigma^+$, the $^5\Pi$ states, and the spin−orbit coupling constant. For the diagonal energies we used the CASPT2 results obtained in the ab-initio calculations for different distances. An isotropic spin−orbit coupling constant that reproduced the ab-initio spin−orbit splittings was chosen, $\lambda = 48$ cm^{-1}. With this crystal field approach all the spin−orbit couplings are constant and independent of the distance in contrast to the ab-initio calculations.

3. Results

First let us comment on the ab-initio results without spin−orbit coupling. For the different methods I−IV (see Compu-

TABLE 2: CASPT2 Energies and Geometries

		without core			with core correlation		
	state	method	R_{min} (Å)	E_{min} (hartrees)	method	R_{min} (Å)	E_{min} (hartrees)
H_0	$^5\Sigma$	(I)	1.841	−1243.086 052	(II)	1.838	−1249.491 987
	$^5\Delta$		1.846	−1243.042 765		1.835	−1249.451 991
	$^5\Pi$		1.808	−1243.077 457		1.798	−1249.486 648
$H_0 + H_{rel}$	$^5\Sigma$	(III)	1.833	−1243.402 984	(IV)	1.830	−1249.808 959
	$^5\Delta$		1.833	−1243.364 017		1.822	−1249.773 475
	$^5\Pi$		1.792	−1243.399 631		1.782	−1249.809 148

tational Details), the total energies for the minima of the different states are given in Table 2. The most important fact is that only when both relativistic terms are included and the core is correlated does $^5\Pi$ become the lowest state. Going from method I to method IV the $^5\Sigma^+$ state increases its energy relative to the $^5\Pi$ and $^5\Delta$ with about 0.01 au (1 au = 219 474.625 cm^{-1}) or about 2000 cm^{-1}. The energy gap between the $^5\Pi$ and the $^5\Delta$ remains constant within a few hundred inverse centimeters for all four methods. However the change in equilibrium distance is large: 0.027 Å for $^5\Pi$, 0.024 Å for $^5\Delta$, and 0.01 Å for Σ^+. The general trend for the three states is that both relativistic effects and core correlation decrease the equilibrium distance, especially for the $^5\Pi$ and $^5\Delta$; further the effects seem to be additive, which also applies for the relative energy increase of the $^5\Sigma^+$ state. At the CASSCF level the energy difference between the $^5\Sigma^+$ and the $^5\Pi$ is much larger; about 10 000 cm^{-1}, with the $^5\Sigma^+$ lowest. Obviously the $^5\Pi$ state recovers more correlation energy than the $^5\Sigma^+$ state in going from CASSCF over CASPT2 to CASPT2+core. This trend suggests that the $^5\Pi$ is the ground state, and it can be expected that the most reliable results are obtained with method IV. In comparison to the experimental equilibrium distance 1.79 Å (ref 3), we can see that for all methods (I−IV) the $^5\Pi$ state is closest. These experiments refer to diffraction measurements in gas phase; they are not a direct measurement of the distance, and it could not be excluded that the structure of the CrF_2 might be bent or distorted as an effect of Renner−Teller coupling.

Next we comment on the effects of the spin−orbit coupling. In crystal field calculations of transition metal complexes,[11] the spin−orbit coupling constant is reduced from its free ion value (typical reduction is 10−30%). The reduction depends on the ligands and the nature of the bond. In our calculations we see the following reductions of orbital angular momenta: from free Cr^{2+} to CrF_2, the matrix element between the (z^2)- and the (xz)-orbital is reduced to 85%; the matrix element between the (x^2-y^2)- and the (xy)-orbital is reduced to 95%; the matrix element between the (xz)- and the (yz)-orbital remains constant.

Let us look at the effect of spin−orbit coupling on the ground state. In Figure 1 we have displayed the CASPT2 energies of the $^5\Sigma^+$, $^5\Pi$, and $^5\Delta$ states before and after spin−orbit coupling with the effective spin−orbit operator. The distance is expressed in angstroms on the x-axis. The minima of the dotted curves relate to method IV, i.e., relativistic corrections + core correlation. In comparison to the spin−orbit splitting, the $^5\Delta \leftarrow {}^5\Sigma^+$ and $^5\Delta \leftarrow {}^5\Pi$ excitation energies are large.

In Figure 2a,b, two different calculations are presented. In both parts of the figure the dotted lines refer to the CASPT2 energies of the $^5\Pi$ and $^5\Sigma^+$ states. The figures show the lowest part of the potential surfaces of the $^5\Sigma^+-{}^5\Pi$ crossing including spin−orbit interaction for ab-initio (Figure 2a) and crystal field calculations (Figure 2b). Both calculations yield virtually identical results, indicating the validity of a d-only model for the spin−orbit coupling.

The $^5\Pi$ ground state is characterized by a calculated equilibrium distance of 1.782 Å. This distance is changed after inclusion of spin−orbit coupling to 1.787 Å. The change in distance of 0.005 Å is small, and the total energy is lowered about 100 cm^{-1} for the lowest spin−orbit state Π. Since the experimental work could not really differentiate between a linear or a bent structure, it is tempting to consider a Renner−Teller type distortion of the spin−orbit coupled doubly degenerate Π state. We performed some trial calculations of the bent structure, but the effect turned out to be small. The bending of the molecule reduces the symmetry to C_{2v}, and the states are

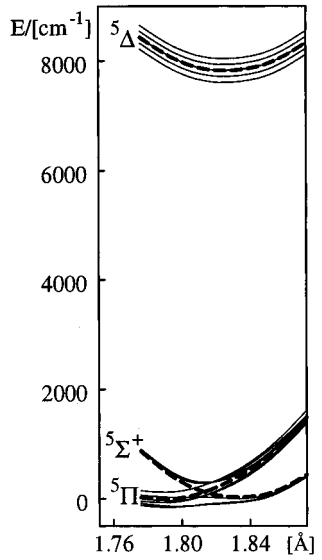

Figure 1. Ab-initio potential energy curves for the $^5\Pi$, $^5\Sigma^+$, and $^5\Delta$ states as a function of the symmetrical stretch. The dotted lines refer to the CASPT2 results with core-correlated and relativistic mass velocity and Darwin terms (method IV) and the solid lines to the effect of one-center effective spin−orbit coupling on the CASPT2 states.

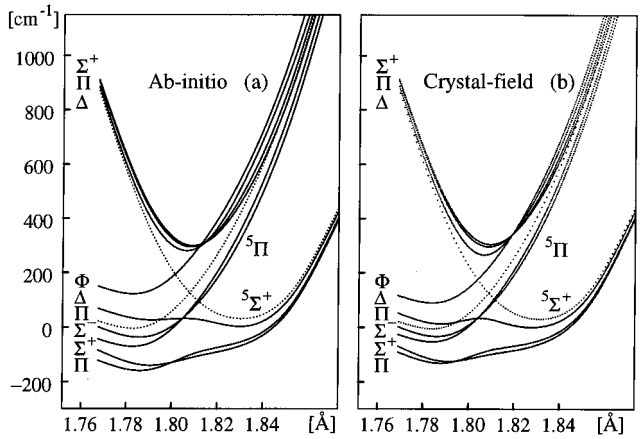

Figure 2. (a) Lower part of Figure 1 enlarged. It contains a curve crossing between the $^5\Pi$ and $^5\Sigma^+$ states (dotted). Each of the solid lines represents spin−orbit states after inclusion of spin−orbit coupling and is labeled with the corresponding double-group symbols Σ^+, Π, Σ^-, Δ, and Φ. (b) Crystal field type calculations of the spin−orbit couplings with λ = 48 cm^{-1}. The diagonal energies of the $^5\Pi$ and the $^5\Sigma^+$ states are the CASPT2 energies from the ab-initio calculations.

resolved as follows: $^5\Sigma_g^+ \rightarrow {}^5A_{1g}$, $^5\Pi_g \rightarrow ({}^5A_{2g} + {}^5B_{2g})$, and $^5\Delta_g \rightarrow ({}^5A_{1g} + {}^5B_{1g})$. As a result orbital mixing between the $^5\Delta_g$ and $^5\Sigma_g^+$ states via the common $^5A_{1g}$ component becomes possible. The mixing leads to a discontinuity in the potential surfaces, which precludes a further study of possible Renner−Teller activity.

Looking in detail at the spin−orbit states in Figure 2 we see some interesting features. The ordering of the spin−orbit states coming from the $^5\Pi$, before and after the crossing with the $^5\Sigma^+$ state, are from below: Π, Σ^+, Σ^- Π, Δ, Φ. For the split $^5\Pi$ the lower states seem to have the lower projection of angular momenta in the *z*-direction. Before and after crossing Σ^+ and Σ^- change place. This can be expected since the $^5\Sigma^+$ contains a Σ^+ state but no Σ^- state. Therefore the Σ^+ states from $^5\Sigma^+$ and $^5\Pi$ will be repelled through the spin−orbit interaction.

There are three "multiplet crossings" (with near accidental degeneracies) occurring at three different distances, a pattern that is nicely reproduced with the crystal field type Hamiltonian. It is possible to draw a line that will intersect all three crossings as well as the crossing before spin−orbit coupling. We suspected this to be reminiscent of atomic spherical symmetry. It has been shown[10,11] that there are indeed cases in octahedral complexes where spherical type transformation properties of the isolated t_{2g} shell will give spin−orbit splitting patterns analogous to atomic splitting patterns. More precisely looking at the effect of the spin−orbit operator acting within the space of the t_{2g} d-orbitals in octahedral symmetry, usually defined as *xy*, *xz*, *yz*, an analogy to atomic p-orbitals can be observed. To show this we transform the t_{2g} shell to another form.

$$\begin{pmatrix} t_{2g}^1 \\ t_{2g}^0 \\ t_{2g}^{-1} \end{pmatrix}_{O_h} = \begin{pmatrix} & Y_{-1}^2 & \\ (1/\sqrt{2}) & (Y_2^2 - Y_{-2}^2) & \\ & -Y_{+1}^2 & \end{pmatrix} \tag{3.1}$$

This complex basis can be put into correspondence with the p-orbitals in spherical symmetry. Expressed in this way the action of the angular momentum operator is proportional to the angular momentum operator for the atomic p-shell, but with opposite sign: $\hat{L}_x^{t_{2g}} = -\hat{L}_x^p$, $\hat{L}_y^{t_{2g}} = -\hat{L}_y^p$, $\hat{L}_z^{t_{2g}} = -\hat{L}_z^p$.

$$\begin{pmatrix} p_1 \\ p_0 \\ p_{-1} \end{pmatrix} = \begin{pmatrix} Y_1^1 \\ Y_0^1 \\ Y_{-1}^1 \end{pmatrix}, \quad \text{with} \quad t_{2g}^{(i)} \leftrightarrow p_i \tag{3.2}$$

Consequently in octahedral symmetry a $^3T_{1g}(t_{2g}^2)$ state, for example, will be split by spin−orbit coupling like an inverted $^3P(p^2)$ atomic state. Following Hund's rule this gives the following order in the atomic state counted from the lowest state, $J = 0, 1, 2$, and in the octahedral, $J' = 2, 1, 0$. Here we use the prime index to underline that the coupling refers to a pseudo angular momentum. In the crossing of the $^5\Sigma^+$ and $^5\Pi$ states in CrF_2 an analogous orbital triplet is formed that can also be related to the atomic case. If the $\sigma^+(d_{z^2})$ and the $\pi(d_{xz},d_{yz})$ orbitals are defined as follows

$$\begin{pmatrix} \pi_1 \\ \sigma_0^+ \\ \pi_{-1} \end{pmatrix}_{D_{\infty h}} = \begin{pmatrix} Y_1^2 \\ Y_0^2 \\ Y_{-1}^2 \end{pmatrix} \tag{3.3}$$

we can see another relation to the atomic p-shell that we will use below, $\hat{L}_x^{D_{\infty h}} = \sqrt{3}\hat{L}_x^p$, $\hat{L}_x^{D_{\infty h}} = \sqrt{3}\hat{L}_y^p$, $\hat{L}_z^{D_{\infty h}} = \hat{L}_z^p$. Unlike the octahedral t_{2g}-shell the sign of the isomorphism is now positive, but there is an anisotropy differentiating the (*x*,*y*)- and the *z*-directions. In the earlier studies of octahedral complexes,[10,11] the t_{2g} shell is considered as separate from other orbitals; all orbitals below are doubly occupied and all above empty. In CrF_2 the situation is more complicated. The σ^+ and the π orbitals can be considered as one shell, but the δ orbitals are now half-filled and have a spin-angular momentum contribution although their orbital-angular momenta add up to zero. As we will show it is possible to apply the pseudo angular momentum theory[10,11] also for this case.

First we consider the CrF_2 $^5\Sigma^+$ and $^5\Pi$ states as composed of two coupled spin systems. This is possible considering that in both cases the δ orbitals are singly occupied and high-spin coupled to the remaining two electrons residing in three orbitals: the two degenerate π and the σ^+. We thus can perform a decomposition of the four electrons in the five d-orbitals into two triplet systems high-spin coupled to give a quintet.

Secondly we will have to couple the resulting spin to the orbital angular momentum. In view of the correspondence with the atomic p^2 system, the coupling at the crossing point can be described as a LS-coupled pseudo state. We just add up the spin-angular momenta and the orbital angular momenta separately. This gives $L' = 1$ and $S = 2$; therefore, $J' = 1, 2, 3$. The normal Hund's rule seems to apply for our pseudo state $^5P'$. The ordering is $J' = 1, 2, 3$ from below, which is expected as the sign of the isomorphism is positive unlike in the octahedral case.

The reason that the crossings occur at different distances is the geometrical factor in the spin−orbit matrix elements. This geometrical factor can be understood as a squeezing of the spherical symmetry, which may be compensated by cylindrical splitting of the $^5\Sigma^+$ and $^5\Pi$ levels. This explains the tilting of the crossing points. It can further be noted that the tilting is more pronounced in the crystal field approximation as compared to the ab-initio results. This reflects the anisotropic reduction of the spin−orbit coupling constant from its free ion value. If the crystal field spin−orbit coupling Hamiltonian is decomposed with different values in the *x*-, *y*-, and *z*-directions, the anisotropy, found in CrF_2 with the ab-initio calculations, would translate to: $\lambda_z < (\lambda_x = \lambda_y)$, with $\lambda_z / \lambda_x = 0.86$.

Finally we would like to discuss the behavior of the crossings as a function of normal mode distortions. It is clear that the combined antisymmetric stretch and bending mode would reduce the symmetry of the molecule to C_s. If such a mode was added as another coordinate, we should see the three intersection points forming the narrow troughs in three conical intersections added diagonally on top of each other. It is interesting to speculate how such a ground state would behave spectroscopically (for a review of nonadiabatic chemistry see ref 1). However it must be kept in mind that the accuracy of the CASPT2 method cannot be assumed to be better than about 1000 cm^{-1}. Whether or not the $^5\Sigma^+$ and the $^5\Pi$ states are virtually degenerate and at about the same equilibrium distance can only be determined through further spectroscopic experimental studies and more refined theoretical work.

4. Conclusions

We have analyzed the ground state of the CrF_2 molecule with ab-initio calculations including spin−orbit coupling and crystal field calculations. The ab-initio results indicated that the ground state is a $^5\Pi$ intersecting closely with a $^5\Sigma^+$ state. The intersection gives rise to an anisotropic pseudo atomic spin−orbit splitting pattern. The pattern follows Hund's rule with the order $J' = 1, 2, 3$. An earlier developed theory of pseudo atomic angular momenta was adapted and applied to explain the splitting pattern.

It might be possible that this molecule possesses an unusual ground state consisting of three conical spin−orbit Renner−Teller intersections added diagonally on top of each other with a spacing of no more than 200 cm^{-1} and shifted in distance about 0.01 Å along the totally symmetric stretch vibration.

Acknowledgment. This work has been supported by grants from the Belgian National Science Foundation (NFWO), the Belgian Governement, and by the European Commision through the TMR program (Grant ERB FMRXCT 960079).

References and Notes

(1) Yarkony, D. R. *J. Phys. Chem.* **1996**, *100*, 18612.
(2) Pierloot, K.; Dumez, B.; Ooms K.; Ribbing, C.: Vanquickenborne, L. G. To be published.
(3) Zasorin, E. Z.; Gershikov, A. G.; Spiridonov, V. P.; Ivanov, A. A. *Zh. Strukt. Khim*. **1988**, *5*, 680.
(4) Andersson, K.; Blomberg, M. R. A.; Fülscher, M. P.; Kellö, V.; Malmqvist, P. Å.; Noga, J.; Olsen, J.; Roos, B. O.; Sadlej, A. J.; Siegbahn, P. E. M.; Urban, M.; Widmark, P-.O. *MOLCAS Version 3 User's guide*; Dept. Chem. Chem. Centre, Univ. of Lund, 1994.
(5) Pierloot, K.; Dumez, B.; Widmark, P.-O.; Roos, B. O. *Theor. Chim. Acta* **1995**, *90*, 87.
(6) Widmark, P.-O.; Malmqvist, P.-Å.; Roos, B. O. *Theor. Chim. Acta* **1990**, *77*, 291.
(7) Ribbing, C.; Odelius, M.; Kowalewski, J. *Mol. Phys.* **1991**, *74*, 1299.
(8) Ribbing, C.; Daniel, C. *J. Chem. Phys.* **1994**, *100*, 6591.
(9) Weissbluth, M. Atoms and Molecules; Academic Press: New York, 1978.
(10) Ceulemans, A. *Top. Curr. Chem.* **1994**, *171*, 27.
(11) Ballhausen, C. Introduction to ligand field theory; McGraw-Hill Book Company: New York, 1962.
(12) Thompson, W. J. *Angular momentum*; John Wiley & Sons inc.: New York, 1994.